FOSL2 truncating variants in the last exon cause a neurodevelopmental disorder with scalp and enamel defects

Auriane Cospain, Ana Rivera-Barahona, Erwan Dumontet, Blanca Gener, Isabelle Bailleul-Forestier, Isabelle Meyts, Guillaume Jouret, Bertrand Isidor, Carole Brewer, Wim Wuyts, et al.

FOSL2 truncating variants in the last exon cause a neurodevelopmental disorder with scalp and enamel defects

Auriane COSPAIN[1,2,#,*], Ana RIVERA-BARAHONA[3,4,*], Erwan DUMONTET[5], Blanca GENER[6], Isabelle BAILLEUL-FORESTIER[7], Isabelle MEYTS[8,9], Guillaume JOURET[10], Bertrand ISIDOR[11], Carole BREWER[13], Wim WUYTS[14], Leen MOENS[8], Selket DELAFONTAINE[8,9], Wayne Wing Keung LAM[15], Kris VAN DEN BOGAERT[16], Anneleen BOOGAERTS[16], Emmanuel SCALAIS[17], Thomas BESNARD[11], Benjamin COGNE[11,12], Christophe GUISSARD[18], Paul ROLLIER[1,2], Wilfrid CARRE[2], Regis BOUVET[2], Karin TARTE[5], Ricardo GÓMEZ-CARMONA[3,4], Pablo LAPUNZINA[19,3], Sylvie ODENT[1,20], Marie FAOUCHER[2,20], Christele DUBOURG[2,20], Víctor L. RUIZ-PÉREZ[3,4], Koen DEVRIENDT[16], Laurent PASQUIER[21,*] , Luis A. PÉREZ-JURADO[22,23,3,#,*]

Affiliations:
[1]Service de Génétique Clinique, Centre de Référence CLAD-Ouest, ERN ITHACA, CHU, Rennes, France
[2]Laboratoire de Génétique Moléculaire et Génomique, CHU, Rennes, France
[3]Centro de Investigación Biomédica en Red de Enfermedades Raras, ISCIII, Madrid, Spain
[4]Instituto de Investigaciones Biomédicas Alberto Sols, CSIC-Universidad Autónoma de Madrid, Madrid, Spain
[5]Laboratoire d'Immunologie - Thérapie Cellulaire et Hématopoïèse, CHU, Rennes, France
[6]Department of Genetics, Cruces University Hospital, Biocruces Bizkaia Health Research Institute, Barakaldo, Spain
[7]Department of Pediatric dentistry, Competence center of rare oral diseases, Faculty of Odontology - Paul-Sabatier University, CHU, Toulouse, France
[8]Laboratory for Inborn Errors of Immunity, Department of Microbiology Immunology and Transplantation KU Leuven, Leuven, Belgium
[9]Department of Pediatrics, University Hospitals Leuven, Leuven, Belgium
[10]National Center of Genetics (NCG), Laboratoire National de Santé (LNS), Dudelange, Luxemburg
[11]Service de Génétique Médicale, CHU de Nantes, Nantes, France
[12]Nantes Université, CHU de Nantes, CNRS, INSERM, institut du thorax, Nantes, France
[13]Department of Clinical Genetics, Royal Devon and Exeter NHS Foundation Trust, Exeter, UK
[14]Department of Medical Genetics, University and University Hospital of Antwerp, Edegem, Belgium
[15]South East of Scotland Clinical Genetics Service, Western General Hospital, Edinburgh, UK
[16]Center for Human Genetics, University Hospitals Leuven–KU Leuven, Leuven, Belgium
[17]Department of Pediatric Neurology, Centre Hospitalier de Luxembourg, Luxemburg
[18]RESTORE Research Center, Université de Toulouse, INSERM 1301, CNRS 5070, EFS, ENVT, Toulouse, France
[19]Instituto de Genética Médica y Molecular (INGEMM)-IdiPAZ, Hospital Universitario La Paz, Madrid, Spain
[20]Univ Rennes, CNRS, IGDR, UMR 6290, Rennes, France
[21]Service de Génétique Clinique, Centre Référence Déficiences Intellectuelles de cause rares, CHU, Rennes, France
[22]Servicio de Genética, Hospital del Mar Research Institute (IMIM), Barcelona, Spain
[23]Department of Medicine and Life Sciences, Universitat Pompeu Fabra, Barcelona, Spain
[*]These authors contributed equally to this work
[#]Correspondence to auriane.cospain@gmail.com or luis.perez@upf.edu

Keywords: FOSL2; FRA-2; aplasia cutis congenita of scalp; enamel hypoplasia; AP-1 complex; Adams-Oliver syndrome

Abstract:

Purpose: We aimed to investigate the molecular basis of a novel recognizable neurodevelopmental syndrome with scalp and enamel anomalies caused by truncating variants in the last exon of the gene *FOSL2*, encoding a subunit of the AP-1 complex.

Methods: Exome sequencing was used to identify genetic variants in all cases, recruited through Matchmaker exchange. Gene expression in blood was analyzed by RT-PCR. *In vitro* co-immunoprecipitation and proteasome inhibition assays in transfected HEK293 cells were performed to explore protein and AP-1 complex stability.

Results: We identified 11 individuals from 10 families with mostly *de novo* truncating *FOSL2* variants sharing a strikingly similar phenotype characterized by prenatal growth retardation, localized cutis scalp aplasia with or without skull defects, neurodevelopmental delay with autism spectrum disorder, enamel hypoplasia and congenital cataracts. Mutant *FOSL2* mRNAs escaped nonsense-mediated mRNA decay. Truncated FOSL2 interact with c-JUN, thus mutated AP-1 complexes could be formed.

Conclusion: Truncating variants in the last exon of *FOSL2* associate a distinct clinical phenotype by altering the regulatory degradation of the AP-1 complex. These findings reveal a new role for *FOSL2* in human pathology.

INTRODUCTION:

FOSL2 (FOS-Like 2) or *FRA2* (FOS-Related Antigen 2), OMIM #601575, is a member of the FOS gene family including *FOS*, *FOSB*, *FOSL1* and *FOSL2*. It encodes a basic region-leucin zipper motif transcription factor that forms part of the activator protein-1 (AP-1) complex, a ubiquitous complex involved in various cellular functions such as proliferation, apoptosis, differentiation, survival and migration[1]. Homodimers and heterodimers associating the JUN, FOS, ATF and MAF protein families, characterized by their highly conserved basic leucine zipper, form this AP-1 complex[1]. In response to extracellular signals (growth factors, hormones, stress, cytokines, inflammation), the protein FOSL2 forms a heterodimer with JUN proteins, and binds to specific DNA binding domains[2]. Binding is dependent on chromatin accessibility and other proteins that orient the position of the heterodimer[3].

FOSL2 has a low tissue specificity with high tissue expression in brain, skin, bone marrow, lymphoid tissues, endocrine tissues, lung, digestive and urologic organs, and the female genital tract[4]. The AP-1 complex has pleiotropic effects during development, including acting as a positive regulator of bone and matrix formation[5–9]. Mice overexpressing *Fosl2* develop an increased bone formation of the entire skeleton[5] as do mice overexpressing the paralog *Fosl1*[7,8]. Conversely, *Fosl2* conditional knock-out (KO, Cre-loxP system, conditional under the coll2a1 promoter) mice showed decreased mineralized bone and calvaria bone, and the complete KO of Fosl2 in embryos and newborn mice was lethal shortly after birth, with severe osteopenia phenotype[9]. Fosl2 was immunolocalized in rat incisor ameloblasts, suggesting a function in enamel formation[10].

A potential role for *FOSL2* in immunological processes has been suggested in the mouse model[7,11]. The AP-1 complex and *FOSL2* are involved in B cells proliferation and differentiation by enhancing transcription factors such as IRF4 (interferon regulatory factor 4, a key factor in the regulation of differentiation of immune cells and required for lymphocyte activation during the immune response[12]) and Foxo1 (Forkhead Box O1, a key factor in the adaptive immune response stimulation, required for B cell differentiation, immunoglobulin rearrangement and class switching[13])[14]. In mice

(conditional KO of Fra-2, restricted to B cells, driving to a theorical homozygous deletion), the deletion of *Fosl2* led to a reduction in numbers of B cells in bone marrow and spleen, and decreased levels of circulating immunoglobulins[14]. Moreover, in mice, *Fosl2* is implicated in inflammatory processes and systemic autoimmunity. Mice overexpressing *Fosl2* exhibit an extensive dermatosis with loss of fur around the eyes and an infiltration of inflammatory cells into multiple organs. This inflammation is T-cell mediated and regulatory T cells (Treg) development is repressed. Conversely, *Fosl2* conditional-KO mice (Cre-LoxP system, conditional for T-cells) show a significant reduction in inflammation severity and autoimmunity[11].

In this study, we report 11 individuals with pathogenic heterozygous variants in the last exon of the gene *FOSL2*. They shared a strikingly similar phenotype of localized scalp aplasia, dental enamel anomalies, and a relatively mild neurodevelopmental disorder. We show how truncated FOSL2 are expressed and lead to increase AP-1 complex stability, likely impairing its appropriate degradation through the proteasome. We propose that a specific category of *FOSL2* variants with dominant effects is associated with a clinically recognizable syndrome.

MATERIALS AND METHODS:

Individuals

Clinical data

A multicentre international matchmaking collaboration, using GeneMatcher[15] along with additional calls through national and international networks including the CIBERER[16] (https://ciberer.es) and the ERN Ithaca (https://ern-ithaca.eu), allowed the collection of biological and clinical data from eleven individuals under follow-up by eight different Genetic Departments. Individuals and/or their parents or legal representatives had given their informed consent for genetic analysis, for sharing of anonymized clinical and molecular information with international collaborators and researchers, and for the publication of the photographs included in the study. This study adheres to the principles set out in the Declaration of Helsinki.

Dental analysis

To explore the three-dimensional microstructure of the sample, tomographic acquisitions were performed with Zeiss Versa 510 laboratory X-ray microscope (Carl Zeiss Meditec) using the procedure described by Dumbryte[17]. To better highlight the structure of the enamel surface, a phase contrast acquisition procedure was carried out. According to the manufacturer's protocol, 1601 projections were acquired and automatically reconstructed with the following parameters: objectif 20x, 1.45µm/px, 140kV, 10W, no filter.

Genetic and expression studies

Exome sequencing and validation

Routine exome sequencing was applied by all genetic services according to their own diagnostic protocols and platforms, either in singletons or in trios (with parents). Candidate mutational events were identified by focusing on protein-altering and splice-site changes supported by >20% of total reads in positions covered by at least 8 reads and absent in population datasets (GnomAD database: https://gnomad.broadinstitute.org/). Sequence reads were aligned to the GRCh37 human reference genome assembly, and *FOSL2* variants are described using the NM_005253.3 reference sequence. For candidate variants of interest, primers were designed to amplify 150-250 bp products centered around the site of interest using default primer3 design settings. PCR products were generated using 100 ng genomic DNA as template. Amplicons were then Sanger sequenced.

Short-term lymphocyte culture (STLC) analysis and gene expression quantification

We established a STLC from blood samples of individual #1. Peripheral blood mononuclear cells (PBMCs) were isolated by Ficoll density gradient-based centrifugation (Lymphoprep™, Axis-Shield) according to a standard procedure. Total RNA was extracted from PBMSCs with NucleoSpin RNA kit (Macherey-Nagel). For reverse transcription, 0.5 µg of RNA and SuperScript™ IV Vilo™ kit (Invitrogen) were used. Prior to reverse transcription (RT) reaction, incubation of RNA samples with ezDNase (Invitrogen) was performed to remove genomic DNA contamination. We performed RT-PCR of *FOSL2* mRNA and Sanger sequencing to assess the level of mutant and wild-type alleles in the

transcripts of probands #1 and #9, using as controls their healthy mothers not carrying the *FOSL2* variant. Semi-quantitative analysis of the mutant to wild-type allele ratios in mRNA was compared to healthy controls by comparative analysis of the peaks after Sanger sequencing for both cases. Quantitative Real-Time PCR was performed for proband #4 and her parents on an AriaMX Real-time PCR system (Agilent) with commercially available Taqman Assays (Applied Biosystems) for *FOSL2* (Hs.00232013_m1) and *GAPDH* (Hs.04420632_g1) genes. Expression values for *FOSL2* were normalized to *GAPDH* expression with three independent technical experiments per sample.

Functional studies

DNA constructs

Wild-type (WT) *Fosl2* (NM_008037.4) and *Jun* (NM_010591.2) cDNAs were PCR amplified from full-length cDNA clones of mouse origin (Source Bioscience) with proofreading hot-start Platinum SuperFi II DNA Polymerase (Invitrogen) and cloned into pLPCX and pEGFP-N1 vectors, respectively. The FLAG-tag sequence was contained within the forward primer of *Fosl2*. *FLAG-Fosl2*-WT plasmid was then used as template to generate the *FLAG*-tagged *Fosl2* Arg199* and Gln207* truncated constructs through PCR amplification using specific reverse primers that included the corresponding mutant nonsense variant. Mutant *FLAG-Fosl2* variants were also inserted into pLPCX vector. All constructs were validated by Sanger sequencing.

Cell culture and Western Blot

HEK293T cells were cultured in Dulbecco's modified Eagle's medium (DMEM) supplemented with 10% fetal bovine serum (FBS) and 1X antibiotic-antimycotic solution: 100 units/ml penicillin, 100 µg/ml streptomycin and 0.25 µg/ml amphotericin B (Gibco, 15240096).

For Western Blot (WB) analysis, cells were washed with PBS and then lysed in RIPA buffer (150 mM NaCl, 50 mM Tris-HCl, 2 mM EDTA, 0.5% sodium deoxycholate, 0.1% SDS, 1% NP-40) supplemented with a protease inhibitor cocktail (Sigma-Aldrich; P8340) and phosphatase inhibitors (Sigma-Aldrich, P0044 and P5726, 1 mM Na_3OV_4 and 10 mM NaF). Protein concentration in cell extracts was determined by the BCA colorimetric assay (Pierce, ThermoFisher Scientific) and WBs were carried out

according to standard protocols[18]. Primary antibodies: anti-FLAG (1:4000; Sigma, F1804), anti-GFP (1:8000; Invitrogen, A6455) and anti-Vinculin (1:2000; Santa Cruz sc-73614). HRP-conjugated secondary antibodies (1:10000) were acquired from Jackson ImmunoResearch. Enhanced chemiluminescence (ECL) reagent (GE Healthcare) was used to develop membranes, which subsequently were exposed to Agfa X-Ray films to detect signal.

Co-immunoprecipitation (Co-IP)

The day before transfection HEK293T cells were seeded at a density of $2.5x10^6$ cells/P100. FLAG-tagged *Fosl2* WT, -Arg199*, -Gln207* or the pFLAG empty vector were co-transfected in a 1:1 proportion with *Jun*-EGFP or pEGFP-N1 empty vector using the calcium phosphate method. A total amount of 2.5 µg of each DNA construct/P100 was used. Cells were lysed 24 hours post-transfection in immunoprecipitation buffer 1X (Dynabeads Co-Immunoprecipitation Kit, Life technologies, 14321D) containing 150 mM of NaCl, protease (Sigma-Aldrich; P8340) and phosphatase inhibitors (Sigma-Aldrich, P0044 and P5726, 1 mM Na_3OV_4 and 10 mM NaF). Subsequently, 200 µg of protein extracts were incubated O/N at 4°C with 10 µl of anti-FLAG (Sigma-Aldrich, M8823) or anti-GFP (ChromoTek, gtma) magnetic beads. After three washes with TBS 1X, beads were boiled in 2X Laemmli buffer containing 100 mM of DTT for 5 min and then processed for Western Blotting.

Proteasome-dependent degradation assay

HEK293T were seeded ($3x10^6$ cells/P100), transfected with 2.5 µg of FLAG-tagged *Fosl2* WT, -Arg199* or -Gln207* as indicated above and cultured for 24 hours. Subsequently, transfected cells were trypsinized and re-plated in a MW6 plate ($1x10^6$ cells/well). Cells were cultured for another 24 hours before treatment with cycloheximide (100 µg/mL) combined with MG132 (10 µM) or its vehicle (DMSO) for 2, 4 or 8 hours, after which were analyzed by Western Blotting.

RESULTS:

A recognizable clinical phenotype:

We report here eleven individuals with truncating variants in *FOSL2* (8 females and 3 males, aged 3 months to 30 years) from ten unrelated families. Clinical data are presented in Table 1 and photographs in Figure 1. For individual #10, clinical information was limited to the presence of scalp aplasia and developmental delay, while little developmental data is still available from another (patient #5), only 6-month-old at the last evaluation. There was no relevant family history in any case, except for individuals #2 and #3 who are sisters with unaffected parents.

The most specific features were the cutis aplasia congenita of the scalp and tooth enamel hypoplasia. All individuals but one (individual #11) had a congenital aplasia cutis of variable size along the midline of the scalp. An underlying skull defect was only mentioned in 4 individuals (#1, #4, #5 and #7). Tooth enamel hypoplasia and discoloration were also reported for 8 out of 9 individuals (all but #11). Individual #1 had a specialist dental consultation. On microscopic analysis, using phase contrast acquisition her canine was compared with a normal primary canine. We observed a hypoplastic area, the subsurface was disassociated in two layers, and enamel was less compact in the canine of the patient (Figure 2).

Other ectodermal particularities were noted: dry skin (3), cutis marmorata (1), small and brittle nails (1), hypotrichosis (1) or hypertrichosis (1), lichen sclerosis (1), and oral features such as late primary and permanent tooth eruption (1), recurrent benign gum tumours (1), early loss of the primary dentition (2), hypodontia (1), and tooth germ deformation (1). Of note, 5 individuals had cataracts, mostly bilateral, either congenital or diagnosed during early childhood.

Six out of 9 individuals had intrauterine growth retardation (IUGR), severe for 5 individuals (birth weight below the 5th percentile). After birth, 5 individuals had a linear growth restriction (#1, #2, #6, #8 and #9). Individual #1 received growth hormone therapy. For individual #2, puberty started at a normal age but was not accompanied by the usual growth spurt, causing a progressive decline of the height percentile. Her brain MRI was normal.

Delayed psychomotor development or intellectual disability (ID) was reported for 7 out of 9 individuals. Mild ID was reported for 4 individuals. The two oldest individuals of this cohort (#9 and

#2, 31 and 20-years-old respectively) had severe ID according to a neuropsychological assessment in adulthood. Motor and language development were delayed for most patients, but first words were spoken before 3-years-old. Autistic spectrum disorder (ASD), with or without attention-deficit hyperactivity disorder (ADHD), was documented for 5 out of 7 individuals. More details about the psychomotor development and neuropsychological profiles are available in supplementary information.

Two individuals (#2 and #9) had seizures. Individual #2 had clinical seizures at 12 days of life, with EEG showing left temporal burst of paroxysmal theta electrical seizures discharges. This focal epilepsy was refractory to phenobarbitone, pyridoxine, pyridoxal phosphate, folinic acid and carbamazepine. At 10-month-old, she underwent a selective left amygdalo-hippocampectomy and thereafter was progressively weaned from anti-epileptic medication. For individual #9, epilepsy started at 14-years-old, and was controlled by carbamazepine and lacosamide, after unsuccessful trials with sodium valproate, oxcarbazepine, lamotrigine, levetiracetam, and perampanel. Electroencephalogram (EEG) was abnormal with poorly organized, irregular, very wide pattern with numerous generalized or diffuse paroxysmal abnormalities, with uncertain left/right dominance. Brain MRI showed a short corpus callosum and a hypotrophic superior vermis.

Immune phenotype was explored in individuals #1, #2 and #9 by immunophenotypic characterization of circulating lymphocytes, study of the reactivity of lymphocytes in response to *in vitro* non-specific activators, and screening of autoreactive antibodies in the patients' serum (Supplementary Table S1). None of the three displayed antinuclear antibody, anti-dsDNA, anti-CCP, rheumatoid factor, hepatic nor neural antibodies. All the blood counts for T, B and NK cells were in the normal range for the three individuals, although two of them displayed a trend towards a rise in memory B cells. These individuals had normal T lymphocyte proliferation assays in response to the different mitogens and antigens.

Truncating variants in the last FOSL2 exon

Whole exome sequencing was performed in the 11 probands. Seven different heterozygous likely gene-disrupting variants (4 frameshift and 3 nonsense) were found, all of them located in the 4th and last exon of *FOSL2* (reference sequence NM_005253.3) (Figure 3A). Several variants were recurrent mutation events in more than one unrelated case (Table 1). Trio analysis, either from exome data and/or ulterior validation by PCR and Sanger sequencing, confirmed the *de novo* mutation occurrence. Individuals #2 and #3, two sisters with unaffected parents, carried the same genetic variant absent in parental blood DNA, suggesting germline mosaicism in a parent. All truncated variants are located proximal to the conserved residues in C-terminal domain of FOS proteins that are targets of phosphorylation and known to be required for AP-1 complex stabilization (Figure 3A).

Mutant mRNA escapes non-sense mediated mRNA decay (NMD)

Transcripts containing premature termination codons (PTCs) usually trigger NMD, a surveillance cellular mechanism that detects and rapidly eliminates transcripts with PTCs to avoid translation into truncated and potentially damaging proteins. However, PTCs that lie in the last exon are predicted to escape from NMD[19]. Since all *FOSL2* variants found introduce PTCs but are consistently located in the last exon of the gene, we hypothesized that mutant mRNAs escape NMD. STLC analysis was performed for the NM_005253.3:c.595C>T p.(Arg199*) variant present in individuals #1, #2 and #3. This analysis showed bi-allelic expression, indicating that the mutant transcript was not subject to NMD. This hypothesis was further investigated by Sanger sequencing of RT-PCR products from blood RNA of individuals #9 and #11, with variants NM_005253.3:c.662_663del p.(Val221Glufs*37) and NM_005253.3:c.810_811del p.(Pro271Cysfs*15), respectively, using their mothers as healthy controls. These analyses showed the approximately equal presence of mutant and wild-type alleles in mRNA for both variants tested (Figure 3C). We also confirmed that global *FOSL2* expression was not affected in individual #4 by quantitative RT-PCR on blood RNA of the proband in comparison with her parents (Figure 3D). Therefore, all tested mutant mRNAs are expressed at least in blood and escape from the NMD pathway. Translation of these mRNAs would result in C-terminally truncated FOSL2, which might possess dominant-negative or deleterious gain-of-function activity[19].

Truncated FOSL2 proteins interact with c-JUN

Since the activator protein 1 (AP-1) transcription factor is assembled from JUN-FOS protein homo- or heterodimers among others, we then studied whether two of the predicted mutant proteins identified in more than one individual (FOSL2 Arg199* and Gln207*) would affect the interaction with c-JUN when co-transfected in a 1:1 proportion in HEK293T cells. Co-immunoprecipitation analysis of protein extracts from transfected cells revealed that both truncated FOSL2 interact with c-JUN, indicating that mutant AP-1 complexes could be formed (Figure 4A-B). The assay also suggests a potential difference in protein stability, with the truncated FOSL2 variants being more stable than the wild type (WT). Moreover, as FOSL2 WT was barely detected in the absence of c-JUN, the interaction of both proteins could slightly improve protein stability (Supplementary Figure S1).

FOSL2 proteins are subjected to proteasome degradation

FOS proteins are short-lived as components of AP-1. The selective degradation of these short-lived proteins in cells is mediated via the ubiquitin-26S proteasome-dependent degradation pathway, which can be efficiently inhibited by the peptide aldehyde MG132 (carbobenzoxy-Leu-Leu-leucinal). To investigate a potential difference in the proteasome-mediated degradation of FOSL2, we treated HEK293T cells transfected with FLAG-tagged *Fosl2* WT, -Arg199* or -Gln207* truncated proteins with cycloheximide (CHX) and MG132 or its vehicle (DMSO). Immunoblot analysis of protein extracts from CHX-treated cells showed that degradation of both WT and truncated variants of FOSL2 was inhibited by MG132 treatment (Figure 4C-D). This result indicates that all FOSL2 variants analyzed in this work are subjected to proteasome-mediated degradation.

DISCUSSION:

Clinical findings

We report here the first clinical and molecular description of a cohort of individuals with truncating heterozygous variants in *FOSL2*. All individuals shared a strikingly similar phenotype characterized by congenital aplasia cutis with or without skull defect, enamel hypoplasia, and a variable

neurodevelopmental delay with ID and/or autistic features. Other reported features include congenital cataracts, prenatal and postnatal growth restriction, and seizures.

Although this cohort is relatively small, we can derive some guidelines for clinical diagnosis and follow up. Firstly, the phenotype is specific enough to be suspected clinically. Differential diagnoses mainly include Adams-Oliver syndrome[20,21], in which congenital aplasia cutis is also one of the key features. However, Adams-Oliver syndrome is distinguishable because it typically includes limb abnormalities (hypoplastic nails, cutaneous or bony syndactyly, transverse reduction defects, ectrodactyly, polydactyly, brachydactyly) and not enamel dysplasia[22]. In one individual, Knobloch syndrome (OMIM #267750), was suggested. This is an autosomal recessive disorder linked to the gene *COL18A1*[23]. In this syndrome, occipital skull defects are associated with encephalocele or occipital cutis aplasia, and ocular features such as congenital cataracts and retinal degeneration. However, dental anomalies are not described in Knobloch syndrome[23–25]. Secondly, the two oldest affected individuals showed some deterioration in neurodevelopmental function, so it would be important to continue to monitor neurological and psychiatric development and progress during childhood and continue into adulthood. Thirdly, we focus about the ophthalmological evaluation at birth and monitoring for congenital cataracts. In one individual (#6) bilateral anterior polar cataracts were not diagnosed until 1-year-old, but were likely to have been present as opacities at birth- and therefore easily missed on routine neonatal screening. Fourthly, individuals should have regular dental follow-up to evaluate enamel dysplasia or possible amelogenesis imperfecta and to minimize symptoms such as pain and increased sensitivity to hot and cold, masticatory difficulties, and aesthetic issues. Early treatment may prevent occlusal wear and improve oral hygiene, thereby minimizing the chance of caries or periodontal disease in primary and secondary dentitions[26].

Molecular basis

FOSL2 is located on chromosome 2, contains 4 exons and codes for a protein of 326 amino acids. *FOSL2* is highly intolerant to heterozygous loss-of-function variants (pLI=0.98, LOEUF=0.24) according to the information in the GnomAD database[27]. The smallest deletion including *FOSL2* reported in the

Decipher database[28] is a 4.80 Megabases heterozygous deletion in 2p23.2 and the associated phenotype combines intellectual disability and dysmorphic features (hypertelorism, abnormal forehead, anteverted nares, long face and wide mouth). This phenotype was not consistent with that described for *FOSL2* truncating variants, which suggests a different mechanism, probably related to haploinsufficiency and/or the involvement of additional genes. A single individual is reported in GnomAD carrying a nonsense variant affecting the main transcript of *FOSL2*, with the variant located in exon 3 and predicted to produce an mRNA that would be subjected to NMD[19]. In our cohort, seven *FOSL2* variants were found in 11 individuals: 4 are frameshift and 3 are nonsense, all located in the last exon. RNA analysis showed the escape of mutant mRNA to NMD, supporting the hypothesis of gain-of-function variants or dominant negative effect of the mutated protein.

Physiopathological hypotheses

FOSL2 differs from other family members in lacking a potent C-terminal transactivation domain and can act to suppress transcription. The sequences that confer the ability to repress onto a heterologous protein are contained within the conserved C-terminal 40 amino acids[29]. However, in heterodimeric combination with JUND, FOSL2 can enhance transcription relative to JUND homodimers, pointing to a critical role in the composition and transactivation potential of the AP-1 complex[29]. In addition, the rate of degradation of the short-lived proteins of AP-1 is important in determining homeostasis and function[30]. We have shown that truncated FOSL2 are produced *in vitro*, all predicted to lack the transrepression domain. These FOSL2 truncated proteins interact with c-JUN, and thereby are able to assemble into mutant AP-1 transcription complexes. In this context, the disease mechanism could be related to an abnormal AP-1 regulation during development affecting several of the processes where AP-1 is important.

Regarding neurodevelopment, abnormal AP-1 activation and impaired neuron-specific chromatin repression has been proposed as the mechanism for the developmental delay and ASD in some patients with BAF pathway variants. Particularly, recessive variants in *ACTL6B* and dominant

SMARCA2 variants can de-repress *FOSL2,* resulting in elevated AP-1 activation and enhancer reprogramming in neural progenitor cells[31,32].

Tooth enamel of individuals with *FOSL2* variants was abnormal at macroscopic level with hypoplastic areas on various teeth associated with visible dentine. This could be due to a weakness of the enamel-dentin junction. At the microscopic level, with phase contrast acquisitions, the enamel subsurface layers are disassociated, and the enamel appears less dense and compact. This phenotype fits within the amelogenesis imperfecta spectrum. *FOSL2* and AP-1 are regulated by the calcitonin gene-related peptide-α (CGRPα), a neurotransmitter involved in bone and tooth formation during development[33,34]. AP-1 is a key player for enamel formation through the regulation of enamel matrix metalloproteinase 20 (MMP-20) expression. MMP-20 is primarily responsible for the initial hydrolysis of amelogenins, main components of the enamel organic matrix, at the secretory and early maturation stages of amelogenesis[35]. Defective MMP-20 proteinase expression would result in a delay in the removal of amelogenins, with a subsequent alteration of enamel matrix mineralization providing an amelogenesis imperfecta (OMIM #612529)[36]. Enamel formation is severely compromised in an MMP-20 knockout mouse model[37].

Aplasia cutis congenita, a rare anomaly characterized by the absence of skin at birth and commonly involving the scalp, is most frequently an isolated condition. It can be associated with additional morphologic abnormalities in ~1/3 of cases, including underlying bony defects, vascular anomalies, or neurologic malformations[38]. The pathophysiologic mechanism is still unknown although many have been suggested causing disruptive development in utero: vascular, genetic, traumatic, pharmacological, or associated with defective neural tube closure. In the case of aberrant FOSL2, a microvasculopathy generated by endothelial cell apoptosis and by reduced endothelial cell migration and chemotaxis[39] might be a contributing factor.

Mouse models overexpressing *Fosl2* showed a pro-inflammatory and autoimmune state, developing a systemic fibrotic disease with increases in dermal thickness, increased myofibroblast differentiation and vascular manifestations. The inflammation was T-cell mediated and Treg development was

repressed. In contract, *Fosl2* KO mice showed a significant reduction of inflammation and autoimmunity[11]. We did not identify any stigmata of autoimmunity in the immunological analyses of three individuals in this cohort. T-cell proliferation and Treg count were normal for the three individuals. An isolated augmentation of unswitched memory B-cell (CD27+IgD+) was found for two out in the three individuals. However, this disproportion in switched/unswitched memory B-cells is frequently observed and does not by itself indicate an immune disease. An extensive study of the individuals' B immune repertoire might be useful to further investigate the immune response linked to *FOSL2*.

The putative mechanism for the congenital cataracts is also unknown. However, AP-1 *cis*-binding motifs are significantly enriched in genes expressed during lens development, suggesting that FOSL2 and AP-1 may have a relevant regulatory role in this process[40].

CONCLUSION:

We show a new role for *FOSL2* in human pathology in a cohort of 11 individuals with a distinct phenotype. All individuals are diagnosed with truncating variants in the last exon of *FOSL2*, altering the normal function of the AP-1 complex.

DATA AVAILABILITY: All data are available upon request to corresponding authors.

ACKNOWLEDGMENTS: We are grateful to Laetitia Pieruccioni and Jacques Rouquette (RESTORE-TRI-GenoToul imaging platform) and Fabrice Schmitt (Carl ZEISS SAS, RMS division) for the enamel analysis and data presentation; the clinicians involved in the patients' clinical care, the biologist, bioinformatics specialist, and technicians; the CIBERER; the ERN-ITHACA; and the families having participated in this study.

ETHICS DECLARATION: Individuals and/or their parents or legal representatives had given their informed consent for genetic analysis, for sharing of anonymized clinical and molecular information with international collaborators and researchers, and for the publication of the photographs included in the study, in accordance with the respective human ethics committees of each participating institution. This study adheres to the principles set out in the Declaration of Helsinki.

FUNDING SOURCES: Research reported in this publication was supported by the Catalonian Department of Health (URDCAT: Grant SLT002/16/00174) and the ENoD Programme of CIBERER (ER16P08), Instituto de Salud Carlos III. Selket Delafontaine is supported by the personal FWO Grant 11F4421N. Isabelle Meyts is a Senior Clinical Investigator at the Research Foundation – Flanders, and is supported by the CSL Behring Chair of Primary Immunodeficiencies, by the KU Leuven C1 Grant C16/18/007, by a VIB GC PID Grant, by the FWO Grants G0C8517N, G0B5120N and G0E8420N and by the Jeffrey Modell Foundation. Part of this work was supported by a grant from the Spanish Ministry of Science and Innovation (PID2019-105620RB-I00/AEI/10.13039/501100011033). The project has also received funding from the European Research Council (ERC) under the European Union's Horizon 2020 research and innovation programme (grant agreement No. 948959). This work is supported by ERN-RITA.

LAPJ is founding partner and scientific advisor of qGenomics Laboratories. The remaining authors declare no potential conflict of interest.

AUTHORS CONTRIBUTIONS:

- Conceptualization: AC, ED, KT, VLRP, CD, KD, LP, LAPJ
- Data curation: AC, ED, LP, CD, KD, LAPJ
- Data Analysis: IB, CG, TB, BC, WC, ED, KT, MF, RB, AB, KVDB, LM, SD, WW, LAPJ, ARB, RGC, PL, VLRP, ES, PR, MF
- Investigation: AC, LP, SO, KD, BI, CB, WL, BG, GJ

- Methodology: KD, LP, KT, VLRP
- Supervision: LP, KD, IM, GJ, BG, BI, CB, LM, WW, SF, WL, KVDB, AB, ES, TB, BC, IBF, CG, WC, KT, ARB, RGC, VLRP, SO, LAPJ, PR, MF
- Validation: AC, ARB, ED, LP, CD, KD, IM, GJ, BG, BI, CB, LM, WW, SF, WL, KVDB, AB, ES, TB, BC, IBF, PR, CG, WC, KT, RGC, VLRP, PL, SO, LAPJ, MF
- Writing – original draft: AC, ED, CD, LP, LAPJ
- Writing – review & editing: AC, LP, IB, CG, KD, LAPJ

LEGENDS:

Table 1: Clinical features of 11 individuals with protein truncating variants in FOSL2. Individual's numbers correspond to those used in the text: #1-5 and #10: nonsense variants; #6-9 and #11: frameshift variants. ASD: autism spectrum disorder; DD/ID: developmental disorder or intellectual disability; F: female; IUGR: intrauterine growth retardation; M: male; NA: data not available; yo: year-old. †Siblings. ††Previously reported and listed in de novo database (https://denovo-db.gs.washington.edu/denovo-db) as c.580_589del10; p.(Pro195Alafs*22)38. †††Ichthyosis vulgaris due to paternally inherited FLG variant.

Figure 1: Craniofacial phenotype. Photographs of the scalp defects, dental anomalies, and facies of eight individuals with FOSL2 variants, including a scan image of the underlying skull defect in individual #7. Numbers are those used in the text and Table 1.

Figure 2: Enamel hypoplasia. Microscopic phase contrast acquisition 20x(1.45µm/px) of the canine of individual #1 (A) compared to a normal primary canine (B). In the hypoplastic area, subsurface is disassociated in two layers in the patient while there is a unique layer in the control (arrows), and enamel is less compact in patient's tooth.

Figure 3: *FOSL2* variants and expression, and escapement to NMD. (**A**) Lollipop plot for *FOSL2* with variants identified in our study. Red lollipops distinguish frameshift variants from orange lollipops for nonsense variants. The green boxes represent the basic leucine zipper domain, formed by the DNA-binding and dimerization domain, and the leucine zipper domain. Transactivation domains in shown by blue boxes and red box represent the transrepression domain. This figure was created with Proteinpaint (https://pecan.stjude.cloud/proteinpaint). (**B**) Location of the truncated variants in relation to the predicted tridimensional structure of FOSL2 (https://alphafold.ebi.ac.uk/entry/P15408). bZIP domain is shown in blue. The location of the

conserved residues that are phosphorylated and thought to be required for regulation of the interaction with c-JUN for AP-1 complex stabilization are marked with asterisks, all located in the carboxy-terminal portion of the protein[30]. (**C**) Sanger sequencing of RT-PCR products from individuals #9 (variant c.662_663del) and #11 (variant c.810-811del) and their healthy mothers, showing the presence of similar amounts of mutant and wild-type alleles (~50%) in whole blood mRNA for both variants tested. (**D**) Quantitative FOSL2 expression by qRT-PCR on whole blood RNA from the proband of family 4 (variant c.619C>T), relative to her unaffected parents, normalized versus GAPDH gene expression. Three independent experiments (represented by circle, square and triangle) were performed for each sample. The means and standard deviations of the three independent technical replicates are shown.

Figure 4: FOSL2 wild type (WT) and truncated variants co-precipitate with c-JUN and are subjected to proteasome degradation. **A-B)** Representative images of anti-FLAG (A) and anti-GFP (B) co-immunoprecipitation (Co-IP) assays in protein extracts from HEK293T cells co-transfected with FLAG-tagged *Fosl2* wild-type (WT), -Arg199* or -Gln207* together with *Jun*-EGFP (n=3 for A and B). Co-IPs with pFLAG (A) and pEGFP (B) empty vectors were used as controls. Immunoprecipitation experiments showed that FOSL2 WT as well as -Arg199* and -Gln207* proteins are all capable to interact with c-JUN. Blots also suggest a potential difference in protein stability between WT and truncated Arg199* and Gln207* variants, being the last two more stable. Longer exposures of the same α-FLAG blots shown in A) and B) are presented in Supplementary Information (Figure S1) for better visualization of FLAG-tagged FOSL2 WT protein in whole cell extracts (input 5%). Plasmids included in each transfection are indicated as +. α-FLAG and α-GFP antibodies were used for FLAG-FOSL2 or c-JUN-EGFP protein detection, respectively. The asterisk designates a nonspecific band. Vinculin (VINC) served as loading control. **C-D)** Protein stability assays of FLAG-tagged FOSL2 WT along with FLAG-tagged FOSL2 -Arg199* (C) or -Gln207* (D) truncated variants transfected in HEK293T cells. Immunoblots showed that incubation with 100 µg/mL cycloheximide (CHX) for 2, 4

and 8 hours reduces the protein levels of both WT and truncated FOSL2 variants and that proteasome inhibition via MG132 (10 μM) restores their expression compared to its vehicle DMSO (n=2). For C) and D), due to differences in FOSL2 levels, distinct amounts of transfected WT (20 μg), Arg199* (4 μg) and Gln207* (2 μg) cell extracts were loaded in gels to avoid signal saturation in the same blot exposure. α-FLAG antibody was used for FLAG-tagged FOSL2 detection. Vinculin (VINC) served as loading control.

REFERENCES:

1. Ye, N., Ding, Y., Wild, C., Shen, Q. & Zhou, J. Small molecule inhibitors targeting activator protein 1 (AP-1). *J Med Chem* **57**, 6930–6948 (2014).
2. Karin, M., Liu, Z. g & Zandi, E. AP-1 function and regulation. *Curr Opin Cell Biol* **9**, 240–246 (1997).
3. Bejjani, F., Evanno, E., Zibara, K., Piechaczyk, M. & Jariel-Encontre, I. The AP-1 transcriptional complex: Local switch or remote command? *Biochim Biophys Acta Rev Cancer* **1872**, 11–23 (2019).
4. Thul, P. J. & Lindskog, C. The human protein atlas: A spatial map of the human proteome. *Protein Sci* **27**, 233–244 (2018).
5. Bozec, A. *et al.* Fra-2/AP-1 controls bone formation by regulating osteoblast differentiation and collagen production. *J Cell Biol* **190**, 1093–1106 (2010).
6. Bozec, A. *et al.* Osteoclast size is controlled by Fra-2 through LIF/LIF-receptor signalling and hypoxia. *Nature* **454**, 221–225 (2008).
7. Wagner, E. F. & Eferl, R. Fos/AP-1 proteins in bone and the immune system. *Immunol Rev* **208**, 126–140 (2005).
8. Jochum, W. *et al.* Increased bone formation and osteosclerosis in mice overexpressing the transcription factor Fra-1. *Nat Med* **6**, 980–984 (2000).
9. Karreth, F., Hoebertz, A., Scheuch, H., Eferl, R. & Wagner, E. F. The AP1 transcription factor Fra2 is required for efficient cartilage development. *Development* **131**, 5717–5725 (2004).

10. Nishikawa, S. Localization of transcription factor AP-1 family proteins in ameloblast nuclei of the rat incisor. *J Histochem Cytochem* **48**, 1511–1520 (2000).

11. Renoux, F. *et al.* The AP1 Transcription Factor Fosl2 Promotes Systemic Autoimmunity and Inflammation by Repressing Treg Development. *Cell Reports* **31**, (2020).

12. Nam, S. & Lim, J.-S. Essential role of interferon regulatory factor 4 (IRF4) in immune cell development. *Arch Pharm Res* **39**, 1548–1555 (2016).

13. Cabrera-Ortega, A. A., Feinberg, D., Liang, Y., Rossa, C. & Graves, D. T. The Role of Forkhead Box 1 (FOXO1) in the Immune System: Dendritic Cells, T Cells, B Cells, and Hematopoietic Stem Cells. *Crit Rev Immunol* **37**, 1–13 (2017).

14. Ubieta, K. *et al.* Fra-2 regulates B cell development by enhancing IRF4 and Foxo1 transcription. *J Exp Med* **214**, 2059–2071 (2017).

15. Sobreira, N., Schiettecatte, F., Valle, D. & Hamosh, A. GeneMatcher: a matching tool for connecting investigators with an interest in the same gene. *Hum Mutat* **36**, 928–930 (2015).

16. Luque, J. *et al.* CIBERER: Spanish national network for research on rare diseases: A highly productive collaborative initiative. *Clin Genet* (2022) doi:10.1111/cge.14113.

17. Dumbryte, I., Vailionis, A., Skliutas, E., Juodkazis, S. & Malinauskas, M. Three-dimensional non-destructive visualization of teeth enamel microcracks using X-ray micro-computed tomography. *Sci Rep* **11**, 14810 (2021).

18. Caparrós-Martín, J. A. *et al.* The ciliary Evc/Evc2 complex interacts with Smo and controls Hedgehog pathway activity in chondrocytes by regulating Sufu/Gli3 dissociation and Gli3 trafficking in primary cilia. *Hum Mol Genet* **22**, 124–139 (2013).

19. Supek, F., Lehner, B. & Lindeboom, R. G. H. To NMD or Not To NMD: Nonsense-Mediated mRNA Decay in Cancer and Other Genetic Diseases. *Trends Genet* **37**, 657–668 (2021).

20. Lehman, A., Wuyts, W. & Patel, M. S. Adams-Oliver Syndrome. in *GeneReviews®* (eds. Adam, M. P. et al.) (University of Washington, Seattle, 1993).

21. Hassed, S., Li, S., Mulvihill, J., Aston, C. & Palmer, S. Adams-Oliver syndrome review of the literature: Refining the diagnostic phenotype. *Am J Med Genet A* **173**, 790–800 (2017).

22. Snape, K. M. G. *et al.* The spectra of clinical phenotypes in aplasia cutis congenita and terminal transverse limb defects. *Am J Med Genet A* **149A**, 1860–1881 (2009).

23. Levinger, N. *et al.* Variable phenotype of Knobloch syndrome due to biallelic COL18A1 mutations in children. *Eur J Ophthalmol* **31**, 3349–3354 (2021).

24. Aldahmesh, M. A. *et al.* Identification of ADAMTS18 as a gene mutated in Knobloch syndrome. *J Med Genet* **48**, 597–601 (2011).

25. Caglayan, A. O. *et al.* Brain malformations associated with Knobloch syndrome--review of literature, expanding clinical spectrum, and identification of novel mutations. *Pediatr Neurol* **51**, 806-813.e8 (2014).

26. Sabandal, M. M. I. & Schäfer, E. Amelogenesis imperfecta: review of diagnostic findings and treatment concepts. *Odontology* **104**, 245–256 (2016).

27. Karczewski, K. J. *et al.* The mutational constraint spectrum quantified from variation in 141,456 humans. *Nature* **581**, 434–443 (2020).

28. Swaminathan, G. J. *et al.* DECIPHER: web-based, community resource for clinical interpretation of rare variants in developmental disorders. *Hum Mol Genet* **21**, R37-44 (2012).

29. Brennan, A., Leech, J. T., Kad, N. M. & Mason, J. M. Selective antagonism of cJun for cancer therapy. *J Exp Clin Cancer Res* **39**, 184 (2020).

30. Gomard, T. *et al.* Fos family protein degradation by the proteasome. *Biochem Soc Trans* **36**, 858–863 (2008).

31. Wenderski, W. *et al.* Loss of the neural-specific BAF subunit ACTL6B relieves repression of early response genes and causes recessive autism. *Proc Natl Acad Sci U S A* **117**, 10055–10066 (2020).

32. Gao, F. *et al.* Heterozygous Mutations in SMARCA2 Reprogram the Enhancer Landscape by Global Retargeting of SMARCA4. *Mol Cell* **75**, 891-904.e7 (2019).

33. Maeda, Y., Miwa, Y. & Sato, I. Distribution of the neuropeptide calcitonin gene-related peptide-α of tooth germ during formation of the mouse mandible. *Ann Anat* **221**, 38–47 (2019).

34. Ren, W. *et al.* Calcitonin gene-related peptide regulates FOSL2 expression and cell proliferation of BMSCs via mmu_circRNA_003795. *Mol Med Rep* **19**, 3732–3742 (2019).

35. Zhang, Y., Li, W., Chi, H. S., Chen, J. & Denbesten, P. K. JNK/c-Jun signaling pathway mediates the fluoride-induced down-regulation of MMP-20 in vitro. *Matrix Biol* **26**, 633–641 (2007).

36. Kim, Y. J. *et al.* Analyses of MMP20 Missense Mutations in Two Families with Hypomaturation Amelogenesis Imperfecta. *Front Physiol* **8**, 229 (2017).

37. Caterina, J. J. *et al.* Enamelysin (matrix metalloproteinase 20)-deficient mice display an amelogenesis imperfecta phenotype. *J Biol Chem* **277**, 49598–49604 (2002).

38. Brackenrich, J. & Brown, A. Aplasia Cutis Congenita. in *StatPearls* (StatPearls Publishing, 2022).

39. Maurer, B., Distler, J. H. W. & Distler, O. The Fra-2 transgenic mouse model of systemic sclerosis. *Vascul Pharmacol* **58**, 194–201 (2013).

40. Zhao, Y., Zheng, D. & Cvekl, A. Profiling of chromatin accessibility and identification of general cis-regulatory mechanisms that control two ocular lens differentiation pathways. *Epigenetics Chromatin* **12**, 27 (2019).

SUPPLEMENTARY INFORMATION:

- **Immunological investigations on three individuals with FOSL2 pathogenic variants:**
- **Neuropsychological assessment and psychomotor development**
- **Longer exposures of α-FLAG blots from figure 4A and 4B for better visualization of FLAG-tagged FOSL2 WT proteins in whole cell extracts (input 5%)**

g.DNA Chr2(GrCh37)		g.28634929C>T	g.28634929C>T	g.28634929C>T	g.28634953C>T	g.28634953C>T	g.28634913_28634923del	g.28634939del	g.28634939del	g.28634996_28634997del	g.28635001C>T	g.28635144_28635145del
c.DNA (NM_005253.3)		c.595C>T	c.595C>T	c.595C>T	c.619C>T	c.619C>T	c.579_589del ††	c.605del	c.605del	c.662_663del	c.667C>T	c.810_811del
p.DNA (NP_005244.1)		p.(Arg199*)	p.(Arg199*)	p.(Arg199*)	p.(Gln207*)	p.(Gln207*)	p.(Ser194Alafs*61)	p.(Pro202Glnfs*18)	p.(Pro202Glnfs*18)	p.(Val221Glufs*37)	p.(Gln223*)	p.(Pro271Cysfs*15)
Case		**#1**	**#2†**	**#3†**	**#4**	**#5**	**#6**	**#7**	**#8**	**#9**	**#10**	**#11**
Sex	8F/3M	F	F	F	F	M	F	F	F	F	M	M
Scalp aplasia cutis/defect	10/11	+	+	+	+	+	+	+	+	+	+	-
Enamel/tooth anomalies	8/9	+	+	+	+	NA	+	+	+	+	NA	-
DD / ID	7/9	Borderline	Mild	-	-	NA	Mild	Severe	Mild	Severe	NA	Mild
IUGR	6/9	+	+	NA	+	-	-	+	+	+	NA	-
Postnatal growth retardation	5/9	+	+	-	-	NA	+	-	+	+	NA	-
ASD	5/9	+	-	-	Selective mutism	NA	+	+	+	-	NA	+
Seizures	2/8	-	+	-	-	NA	-	NA	-	+	NA	-
Eyes	5/10	-	-	-	Congenital bilateral cataracts	Unilateral cataract at 4 m	Bilateral cataracts at 1 yo	Congenital bilateral cataracts	Congenital bilateral cataracts	-	NA	-
Other features										Short corpus callosum and cerebellar vermis hypoplasia. Ichthyosis vulgaris†††		

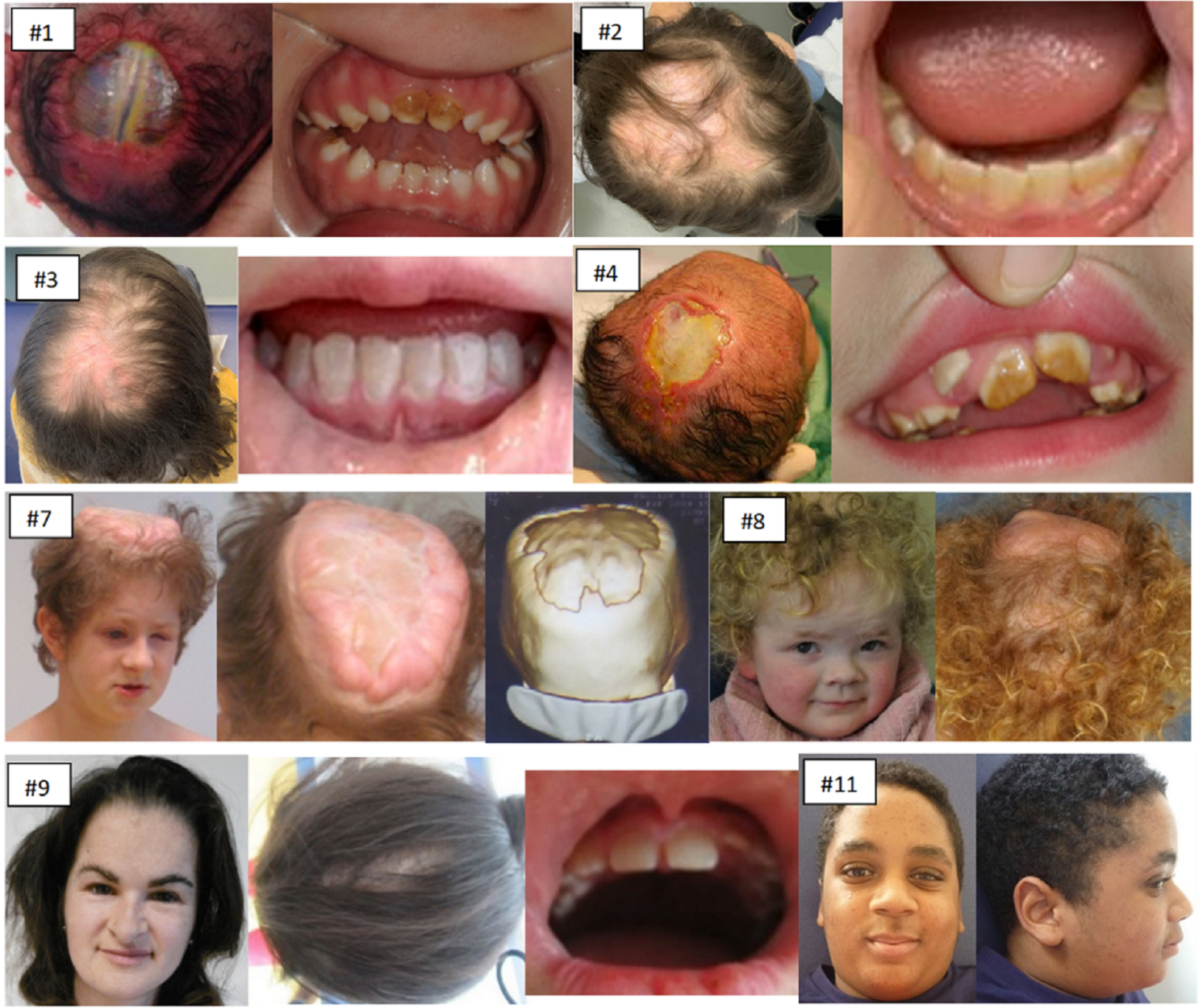
#1
#2
#3
#4
#7
#8
#9
#11

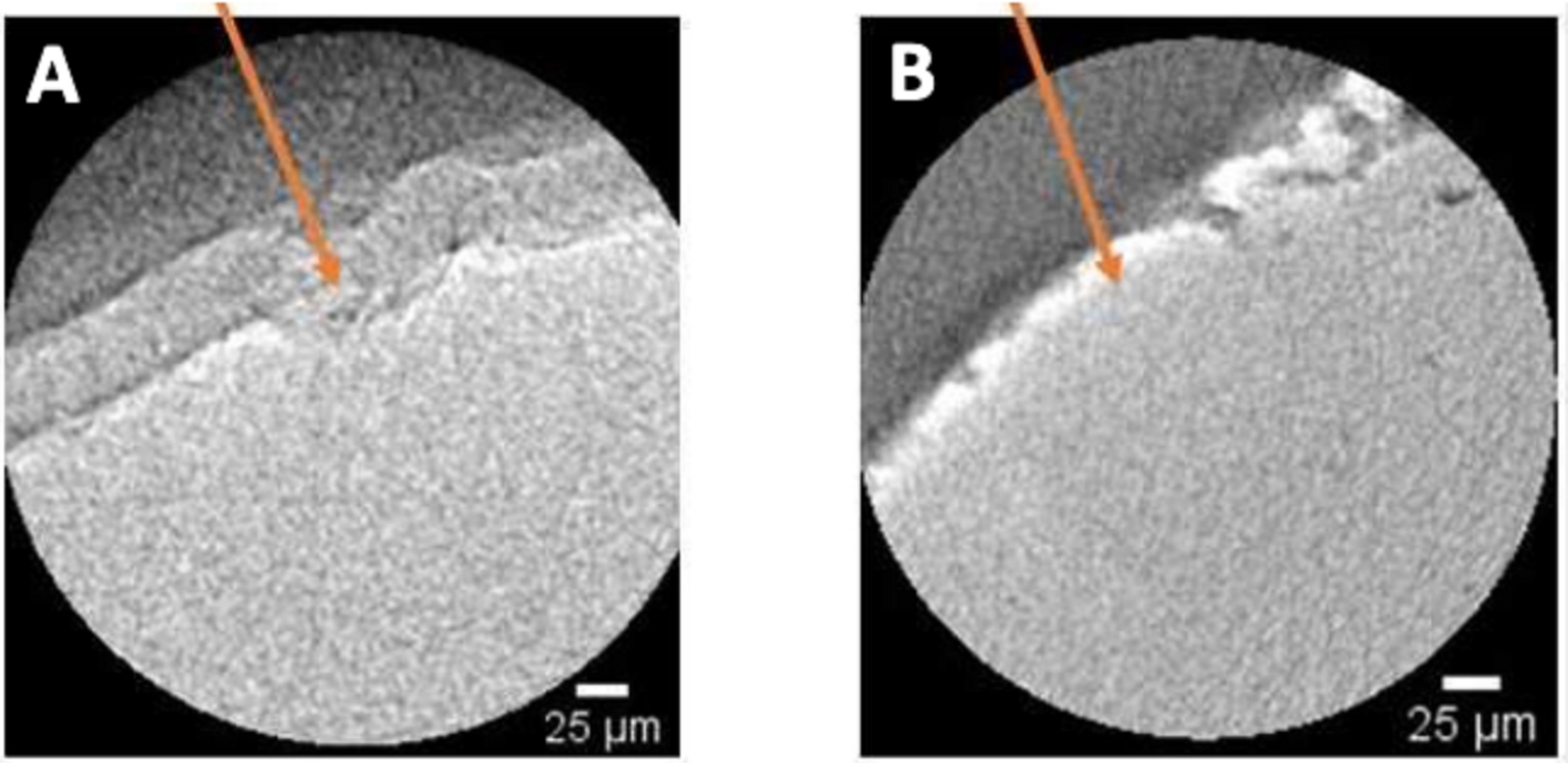
A
25 µm
B
25 µm

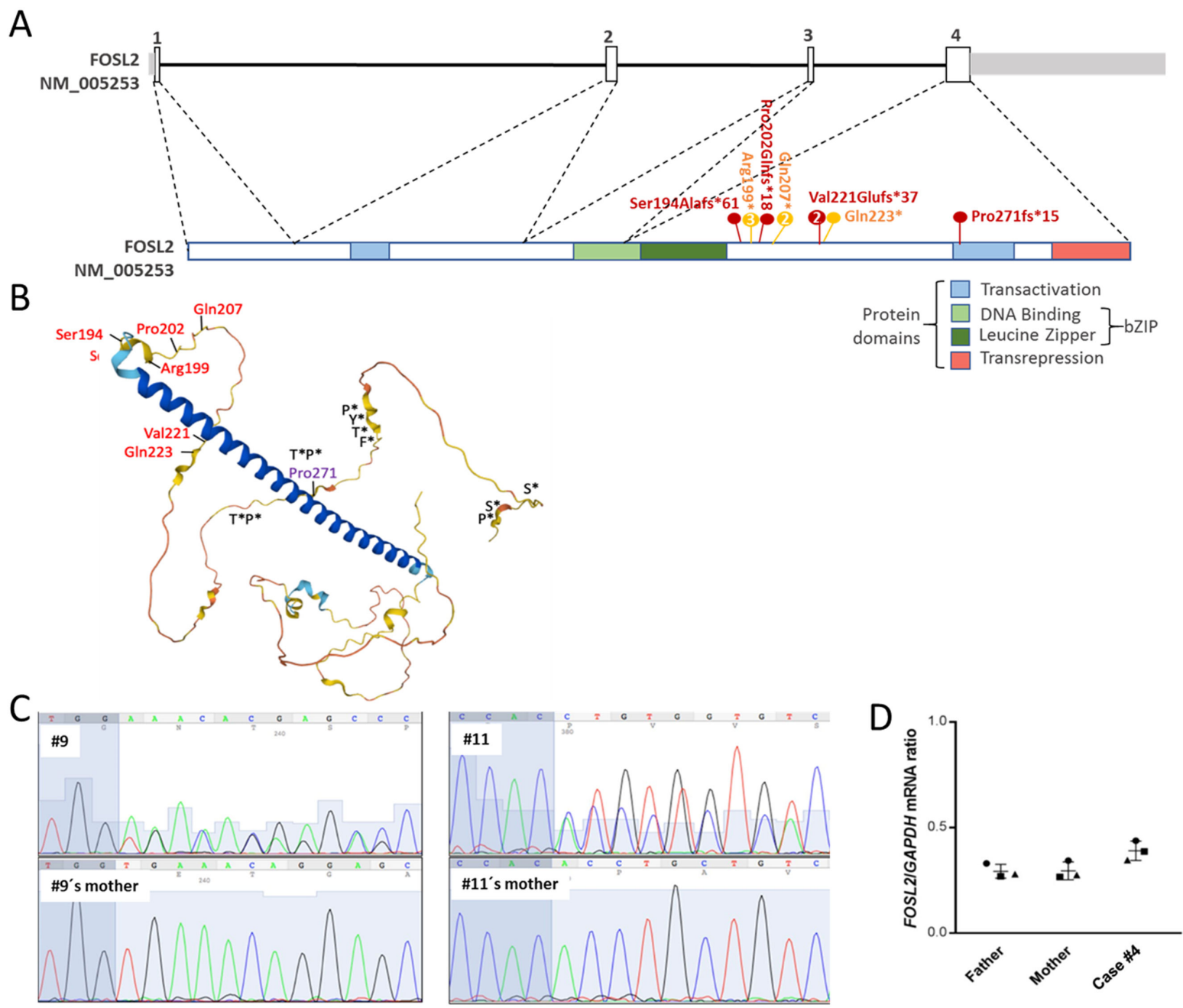
A
1
2
3
4
FOSL2
NM_005253
Arg199*
Rro202Glnfs*18
Gln207*
Ser194Alafs*61
Val221Glufs*37
Gln223*
Pro271fs*15
FOSL2
NM_005253
B
Gln207
Ser194
Pro202
Arg199
Val221
Gln223
T*P*
Pro271
T*P*
P*
Y*
T*
F*
S*
S*
P*
Protein domains
Transactivation
DNA Binding
Leucine Zipper
Transrepression
bZIP
C
#9
#9´s mother
#11
#11´s mother
D
FOSL2/GAPDH mRNA ratio
1.0
0.5
0.0
Father
Mother
Case #4

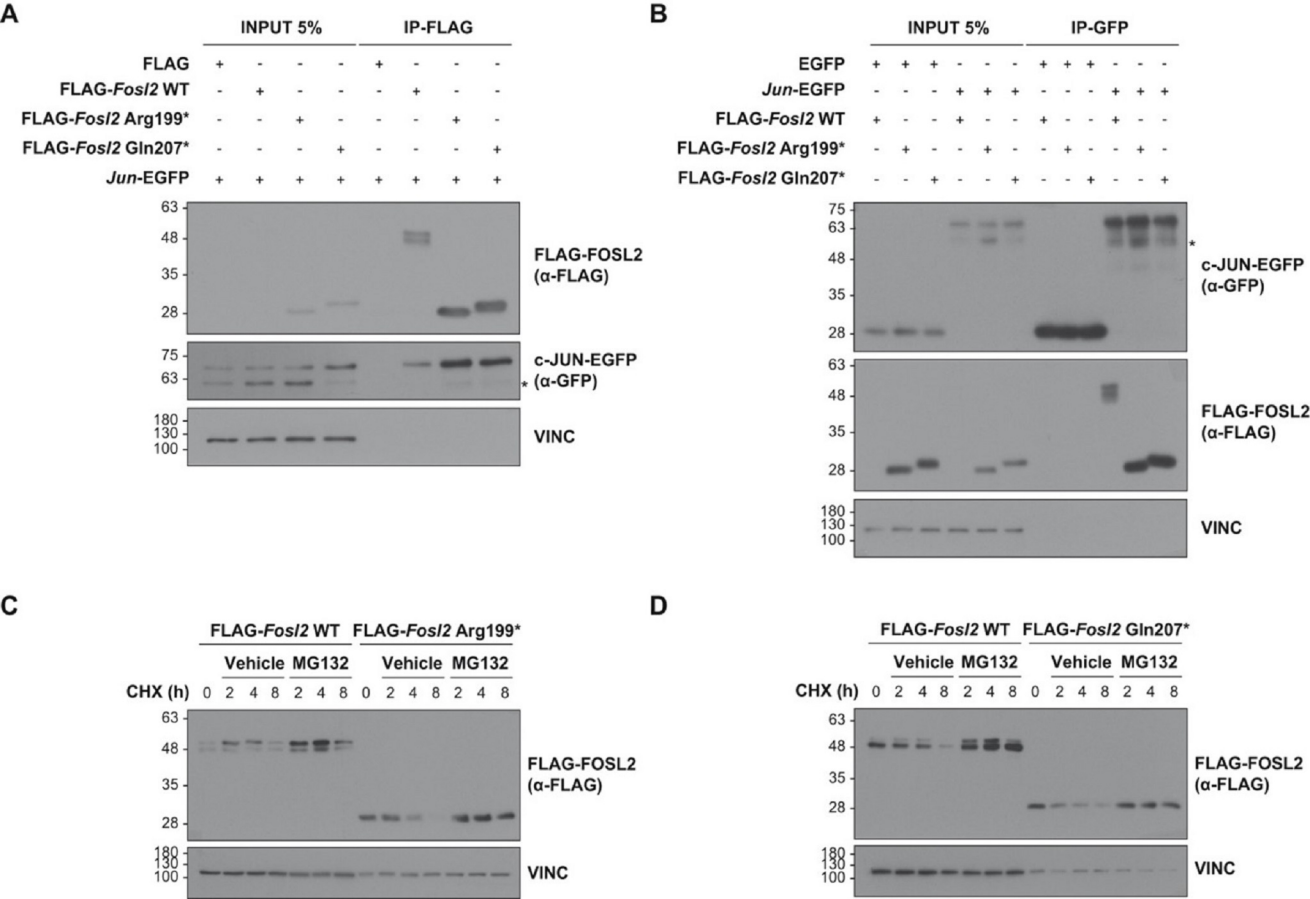
A
INPUT 5%
IP-FLAG
FLAG
FLAG-Fosl2 WT
FLAG-Fosl2 Arg199*
FLAG-Fosl2 Gln207*
Jun-EGFP
63
48
35
28
FLAG-FOSL2
(α-FLAG)
75
63
c-JUN-EGFP
(α-GFP)
*
180
130
100
VINC
B
INPUT 5%
IP-GFP
EGFP
Jun-EGFP
FLAG-Fosl2 WT
FLAG-Fosl2 Arg199*
FLAG-Fosl2 Gln207*
75
63
48
35
28
c-JUN-EGFP
(α-GFP)
*
FLAG-FOSL2
(α-FLAG)
180
130
100
VINC
C
FLAG-Fosl2 WT
FLAG-Fosl2 Arg199*
Vehicle
MG132
Vehicle
MG132
CHX (h)
0 2 4 8 2 4 8 0 2 4 8 2 4 8
63
48
35
28
FLAG-FOSL2
(α-FLAG)
180
130
100
VINC
D
FLAG-Fosl2 WT
FLAG-Fosl2 Gln207*
Vehicle
MG132
Vehicle
MG132
CHX (h)
0 2 4 8 2 4 8 0 2 4 8 2 4 8
63
48
35
28
FLAG-FOSL2
(α-FLAG)
180
130
100
VINC